

# Effect Of Temperature On SnZnSe Semiconductor Thin Films For Photovoltaic Application

Ikhioya I. Lucky<sup>1,2,3</sup>, Okoli D. N<sup>3</sup>, Ekpunobi A. J<sup>3</sup>

<sup>1</sup>Crystal Growth/Material Characterization Laboratory, University of Nigeria, Nsukka

<sup>2</sup>Department of Physics and Astronomy, Faculty of Physical Sciences, University of Nigeria, Nsukka, Enugu State.

<sup>3</sup>Department of Physics and Industrial Physics, Faculty of Physical Sciences, NnamdiAzikiwe University, Awka, Anambra State

## Abstract

In this research we study effect of temperature on SnZnSe semiconductor thin films for photovoltaic application via electrochemical deposition technique using the cationic precursor, which was an aqueous solution of 0.035 mol solution of  $ZnSO_4 \cdot 7H_2O$  while the anionic precursor was 0.1mol solution of selenium metal powder was prepared by dissolving with 4ml of Hydrogen chloride (HCl). The XRD of the films deposited on FTO substrates at different temperature 50°C, 60°C, 70°C and 80°C shows the reflection peaks at (220), (221), (300), (310), (311), (222) and (320) which correspond to the following angle respectively (26.00°), (31.00°), (32.00°), (34.03°),

(37.82°), (51.80°) and (66.00°) are indexed to face-centred cubic structure of SnZnSe with the lattice constant of  $a = 7.189 \text{ \AA}$ . SEM shows random distribution of tiny nano-grains on the substrate, the nano grains were observed to agglomerate due to the presence of large free energy characteristic of small particles. As the temperature of the solution increases from 50°C, 60°C, 70°C, and 80°C the nano grain become more packed. The optical band gap of the deposited material increases from 2.0 – 2.3 eV.

**Keyword:** Electrochemical deposition, FTO, Dopant concentration, Thin film and  $SnCl_2 \cdot 2H_2O$

## I. INTRODUCTION

Zinc selenide (ZnSe) shows unique optical properties exhibiting some potential applications, such as blue-green light emitting diodes, photo-luminescent and electro-luminescent devices, lasers, thin film solar cell, nonlinear optical crystal and infrared optical material [1-2]. ZnSe and its lattice matched ternary alloys have been regarded as useful II–VI compound semiconductors for optoelectronic and photo electronic devices. For the energy ranges from visible to ultraviolet, ZnSe based materials are structured the first manifestation of the blue-green laser in 1991 [3-4]. ZnSe has been a material of choice for blue diode lasers and photovoltaic solar cells since its bulk band gap is 2.7 eV, which can be tuned by adding impurities [5-6]. Out of varieties of applications, ZnSe can be used as optically controlled switching devices [7-8]. Hence it is of great interest as a model material as thin film, quantum wells, bulk crystals and nanodots. Since last few decades the nanosized materials have been subject of great interest due to their unique physical and

chemical properties. Thus the strong, size-dependent optical emission of many semiconductor nanostructures makes them promising candidates for use as fluorescent tags in the study of biological systems. Over the years, ZnSe thin films have been obtained by several preparation approaches including sputtering [9-10], molecular beam epitaxy [11], pulsed laser deposition [12], chemical vapor deposition [13], successive ionic layer adsorption and reaction [14], spray pyrolysis [15], chemical bath deposition (CBD) [16-17] and electrodeposition [18]. Among these techniques, electrochemical deposition offers several advantages: it is relatively economical; it can be used on a large scale. In this research, we reported on effect of temperature on SnZnSe semiconductor thin films for photovoltaic application, in order to study kind of transitions on the structural, morphological and optical properties and the elemental composition of the deposited material for photovoltaic application.

## II. MATERIALS AND METHOD

The chemicals used for this research were analytical grade and they were purchased from Sigma-Aldrich. The growth of SnZnSe thin film semiconductor material included Zinc tetraoxosulphate (VI)

heptahydrate ( $ZnSO_4 \cdot 7H_2O$ ), Tin (II) chloride dehydrate ( $SnCl_2 \cdot 2H_2O$ ), Selenium metal powder (Se), Hydrogen Chloride (HCl). Electrochemical deposition technique (ECD) was used for this research which

involves the deposition of any substance on an electrode as a result of electrolysis which is the occurrence of chemical changes owing to the passage of electric current through an electrolyte. This process involves oriented diffusion of charged growth species through a solution when an external field is applied and reduction of charged growth species at the growth or deposition which also serves as an electrode. The electrochemical bath system is composed of a source of cation (i.e

$\text{SnCl}_2 \cdot 2\text{H}_2\text{O}$ ,  $\text{ZnSO}_4 \cdot 7\text{H}_2\text{O}$  for  $\text{Sn}^{2+}$ ,  $\text{Zn}^{2+}$ ), a source of anion (i.e Selenium metal powder for  $\text{Se}^{2-}$ ), deionized water all in 100ml beaker, magnetic stirrer was used to stir the reaction bath. A power supply was used to provide electric field (DC voltage), a conducting glass was used as the cathode while the anode was carbon and fluorine electrode. Finally, uniform deposition of thin films by electrochemical deposition technique was achieved.

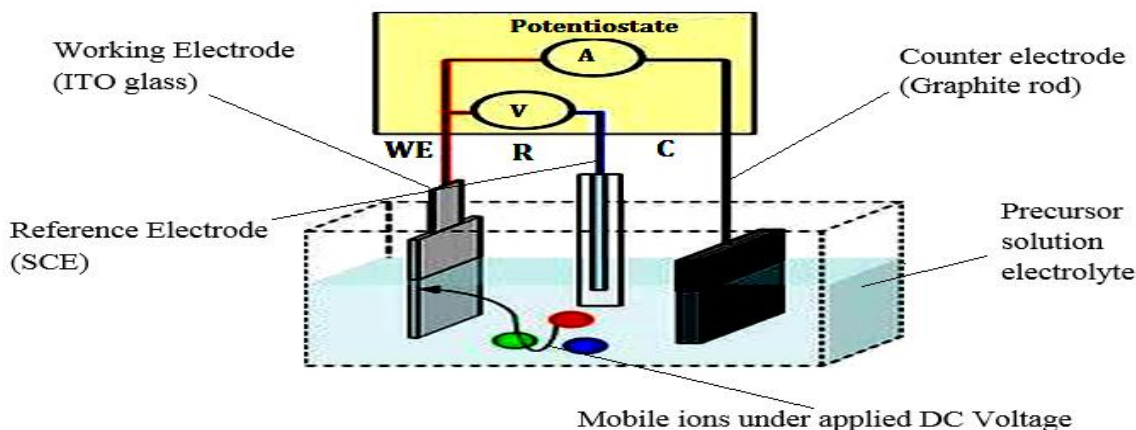


Fig. 1: Schematic diagram of electrochemical deposition technique

#### A. Substrate cleaning procedure

Attention was paid on the cleaning and activating the substrate surface. The selection of the substrate and methods used for the cleaning of the surface of the substrate are very important in the formation of thin films with reproducible process. Nature of the material, size, surface roughness and cleanliness of the substrate play an important role in the formation of the film and its properties such as adhesion, pin-hole density, porosity, film microstructure, morphology and mechanical properties. Substrate cleaning usually involves removing surface contaminations like greasy particles, dust, metals etc. The cleaning process varies with the substrate being cleaned. The contaminants present in the surface of the substrate can be broadly categorized into two types, namely organic and inorganic. Organic contaminants can be easily removed by emulsifying the surface of the substrate with washing solutions. However, for the removal of inorganic contaminants a direct mechanical approach is

needed when they are in particle form. A number of procedures are available for this purpose such as immersing in solvents, ultrasonic cleaning, electronic discharge etc. The systematic procedure used for cleaning the substrates is; Transparent Fluorine doped tin oxide (FTO) coated glass substrates with a sheet resistance of  $10\Omega/\text{m}$  was used as substrate for deposition. The glass substrates were coated only on one side and this conducting side of the glass was detected by the use of a digital multimeter which gave reading as the non-conducting side does not give any reading for the deposition of thin films materials. Hand gloves were used to handle the substrates to avoid contamination. The substrates were dipped in acetone, methanol, rinsed with distilled water and later ultrasonicated for 30min in acetone solution after which they were rinsed in distilled water and kept in an oven to dry. All the prepared substrates were kept in air-tight container.

#### B. The growth of SnZnSe thin films

The growth of SnZnSe thin films materials was carried out using the cationic precursor which was an aqueous solution of 0.035 mol solution of  $\text{ZnSO}_4 \cdot 7\text{H}_2\text{O}$  while the anionic precursor was 0.1mol solution of selenium metal

powder was prepared by dissolving with 4ml of Hydrogen chloride (HCl). This was to ensure a uniform deposition. The electrochemical deposition bath system is composed of a source of cation  $\text{SnCl}_2 \cdot 2\text{H}_2\text{O}$ ,

ZnSO<sub>4</sub>·7H<sub>2</sub>O for Sn<sup>2+</sup>, Zn<sup>2+</sup>), a source of anion (i.e. Selenium metal powder for Se<sup>2-</sup>), distilled water all in 100 mL beaker, and a magnetic stirrer which was used to stir the reaction bath. A power supply was used to provide electric field (DC voltage), a Fluorine doped tin

oxide (FTO) was used as the cathode while the anode was carbon and fluorine electrode. The temperature of the precursor varies in the process of the experiment (See table 1) for detailed.

**Table 1: Variations of growth materials**

Sample	SnCl <sub>2</sub> ·2H <sub>2</sub> O (ml)	ZnSO <sub>4</sub> ·7H <sub>2</sub> O (ml)	Se (ml)	Temperature (O <sup>0</sup> C)	Time (Sec)	Voltage (V)
TT1	10	20	20	50	25	10
TT2	10	20	20	60	25	10
TT3	10	20	20	70	25	10
TT4	10	20	20	80	25	10

**C. Characterization Of The Films.**

The growth films were characterized for their optical properties, electrical properties, Scanning electron microscope and structural properties. The structural characterization of the films was carried out using Bruker D8 Advance X-ray diffractometer with Cu K $\alpha$  line ( $\lambda = 1.54056\text{\AA}$ ) in  $2\theta$  range from 10° - 90° the instrument helped in determining the type of lattice crystal and intensities of diffraction peaks, with the help of data base software supplied by the international center of diffraction data. The quantitative analysis of the films were carried out using Energy Dispersive X-ray Analysis (EDX) for the thin films to study the stoichiometry of the film. This unit is attached to the Zeiss Scanning electron microscope (SEM). When a beam of electrons strikes the specimen, some of the incident electrons excite the atom of the specimen which emits X-ray on returning to the ground state. The energy of the X-ray is related to the atomic number of the excited element. Lithium drifted Si-diode, held at liquid nitrogen temperature is used as a detector of the X-rays. JEOL-JSM 7600F Japan was employed in the present investigation. The electrical characterizations of the films were measured using a four point probe. The

absorbance spectral of the films was obtained in UV-visible NIR using UV-1800 visible spectrophotometer. UV-visible spectrophotometer uses the principle that when a beam of electromagnetic radiation of initial flux I is incident on a transparent object, it is transmitted. Some part of the incident flux could be absorbed for an absorbing medium while some part could be reflected. Various other parameters from the absorbance include: Transmittance, Reflectance, Refractive index, Optical Thickness, Coefficient of absorption, Extinction coefficient, Optical conductivity and dielectric constants were derived using the formula below

(a) From the law of conservation of energy we obtained,

$$A + T + R = 1 \tag{1}$$

Where A is the absorbance, R is the Reflectance, and T is the transmittance.

**III. RESULTS AND DISCUSSION**

**A. Structural Analysis Of SnZnSe Thin Films**

The XRD pattern of SnZnSe thin films deposited on FTO substrates at different temperature 50<sup>0</sup>C, 60<sup>0</sup>C, 70<sup>0</sup>C and 80<sup>0</sup>C. From fig. 4.120, the reflection peaks shown at (220), (221), (300), (310), (311), (222) and (320) which correspond to the following angle respectively (26.00<sup>0</sup>), (31.00<sup>0</sup>), (32.00<sup>0</sup>), (34.03<sup>0</sup>), (37.82<sup>0</sup>), (51.80<sup>0</sup>) and (66.00<sup>0</sup>) are indexed to face-centred cubic structure of SnZnSe [JCPDS card no. 01-

088-2345] reported by [17-19, 23-24] and there is no reported research findings on SnZnSe before this report. The un-indexed peaks could have possibly resulted from the FTO substrates used for deposition. The lattice constant  $a = 7.189\text{\AA}$  was obtained using (equ. 2). From Fig. 2 the higher peaks could be resulted to the fact that the films thickness increases with increase in temperature, thus creating larger surface area for

photovoltaic devices and solar cell activities. The average crystallite size of the films was determined using the Debye-Scherrer's formula. (equ. 3). See table 2 for the calculated crystallite or grain sizes and dislocation density for the films deposited at different temperature 50°C, 60°C, 70°C and 80°C.

Where D stands for the average crystallite size,  $\lambda$ , the wavelength of the X-ray source (0.15416nm),  $\beta$  is the angular line width at half maximum intensity in radians;  $\theta$  is the angle between the incident beam and the scattering plane. The constant of proportionality K is the Scherrer constant which depends on how the width is determined, the shape of the crystal and the size distribution. Although the shape of the crystallites is usually irregular; we can often approximate them as spheres, parallelepipeds, prisms or cylinders. The value of the Scherrer constant K for spherical crystals and parallelepiped like ours is 0.94 [33]. The value of the Scherrer constant K, was estimated as 0.94 for crystallite size using equation (4)

$$d = \frac{n\lambda}{2\sin\theta} \tag{2}$$

$$D = \frac{0.94\lambda}{\beta\cos\theta} \tag{3}$$

$$K = 2\left(\frac{\ln}{\lambda}\right)^{\frac{1}{2}} = 0.94 \tag{4}$$

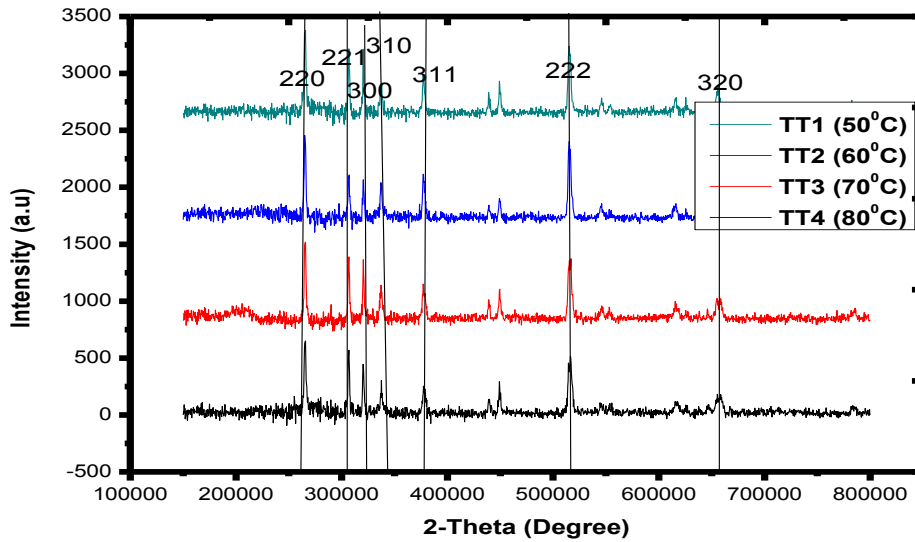


Fig. 2: XRD pattern of SnZnSe deposited at different temperature

Table 2: Structural parameters of SnZnSe thin film deposited at different temperature

Sample	2θ (degree)	d (spacing) Å	Lattice constant (Å)	(β) FWHM	(hkl)	Grain Size(D) nm	Dislocation density, σ lines/m <sup>2</sup>
TT1 (50°C)	26.00	3.52076	7.189	0.60351	220	2.46268	0.16488
	31.00	2.96364		0.60351	221	2.49012	0.16127
	32.00	2.87334		0.60351	300	2.49626	0.16047
	34.03	2.70656		0.60351	310	2.50940	0.15880
	37.82	2.44382		0.60351	311	2.53645	0.15543
	51.80	1.81317		0.60351	222	2.66749	0.14053
	66.00	1.45417		0.60351	320	2.86115	0.12215

TT2 (60 <sup>0</sup> C)	26.00	3.52076	7.189	0.60835	220	2.44308	0.16754
	31.00	2.96364		0.60835	221	2.47031	0.16386
	32.00	2.87334		0.60835	300	2.47640	0.16306
	34.03	2.70656		0.60835	310	2.48943	0.16136
	37.82	2.44382		0.60835	311	2.51627	0.15793
	51.80	1.81317		0.60835	222	2.64626	0.14280
	66.00	1.45417		0.60835	320	2.83838	0.12412
TT3 (70 <sup>0</sup> C)	26.00	3.52076	7.189	0.60931	220	2.43923	0.16807
	31.00	2.96364		0.60931	221	2.46642	0.16438
	32.00	2.87334		0.60931	300	2.47250	0.16357
	34.03	2.70656		0.60931	310	2.48551	0.16187
	37.82	2.44382		0.60931	311	2.51231	0.15843
	51.80	1.81317		0.60931	222	2.64209	0.14325
	66.00	1.45417		0.60931	320	2.83391	0.12451
TT4 (80 <sup>0</sup> C)	26.00	3.52076	7.189	0.60460	220	2.45824	0.16548
	31.00	2.96364		0.60460	221	2.48563	0.16185
	32.00	2.87334		0.60460	300	2.49176	0.16105
	34.03	2.70656		0.60460	310	2.50487	0.15937
	37.82	2.44382		0.60460	311	2.53188	0.15599
	51.80	1.81317		0.60460	222	2.66268	0.14104
	66.00	1.45417		0.60460	320	2.83391	0.12451

### B. Surface Morphology Analysis Using Scanning Electron Microscopy (SEM) of SnZnSe

From fig. 3 shows the surface morphology of SnZnSe thin film grown on fluorine doped tin oxide (FTO) substrates at different temperature of 50<sup>0</sup>C, 60<sup>0</sup>C, 70<sup>0</sup>C, and 80<sup>0</sup>C. It shows random distribution of tiny nano-grains on the substrate, the nano grains were observed to agglomerate due to the presence of large free energy characteristic of small particles. As the temperature of the solution increases from 50<sup>0</sup>C, 60<sup>0</sup>C, 70<sup>0</sup>C, and 80<sup>0</sup>C the nano grain become more packed. The grown

films were homogeneous without cracks indicating uniform deposition and the films cells will act as a good material that will absorb energy from the sun and the cells can also serve as a photovoltaic device and others application in the electronic industry. It was also notices that SnZnSe can be use in mass production of solar cells for the fabrication of lasting solar panel for alternative energy supply [4, 7, 17, 23-24].



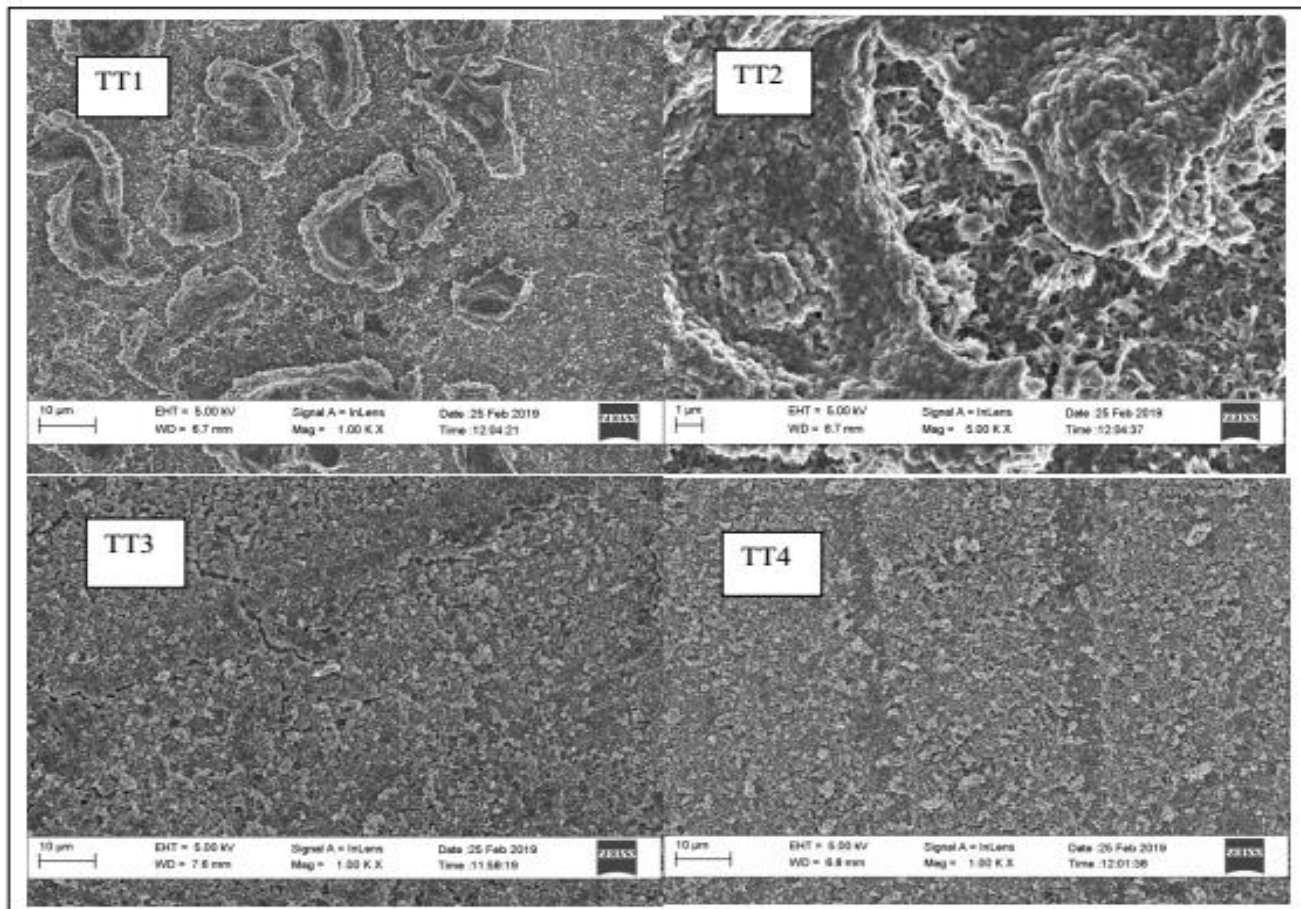


Fig.3: SEM Micrograph of SnZnSe

**C. Elemental Composition Analysis Using Energy Dispersive X-Ray (EDX) for SnZnSe**

The formation of SnZnSe are evident in fig. 4 in the EDX spectra analysis and the others element present is due to the elemental composition of the (FTO)

substrate used for the deposition of the films

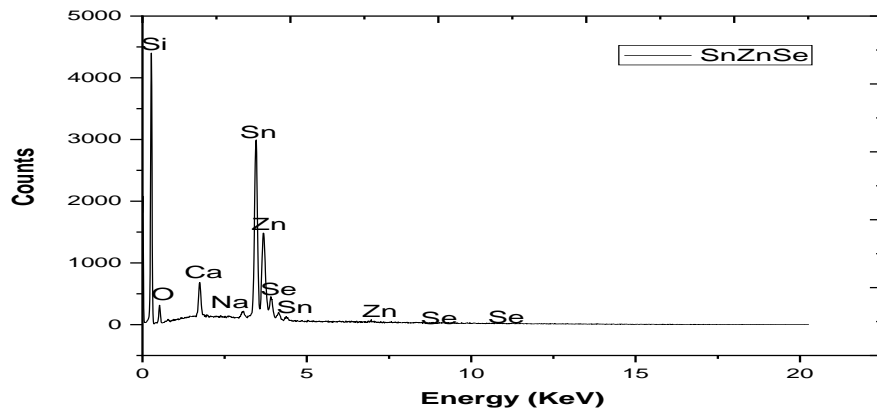


Fig. 4: EDX spectra of SnZnSe.

**D. Optical study of SnZnSe**

The optical absorbance of SnZnSe thin films shown in fig. 5 spectral shown that the films grown under the same parametric conditions at varies deposition temperature (50<sup>0</sup>C, 60<sup>0</sup>C, 70<sup>0</sup>C and 80<sup>0</sup>C) for sample TT1, TT2, TT3 and TT4 reveal that as the wavelength of the incident radiation of the material increase the absorbance of the material decreases. It was observed that as temperature of the grown material increase from 50<sup>0</sup>C - 80<sup>0</sup>C the absorbance of the materials decreases

which reveals the absorbance of SnZnSe cells grown will be a good material that will absorb energy from the sun[4, 7, 17-19, 23-24] and there is no reported research findings on SnZnSe before this report. SnZnSe cells can also serve as a photovoltaic device and others application in the electronic industry. It was also notices that SnZnSe can be use in mass production of solar cells for the fabrication of lasting solar panel for alternative energy supply.

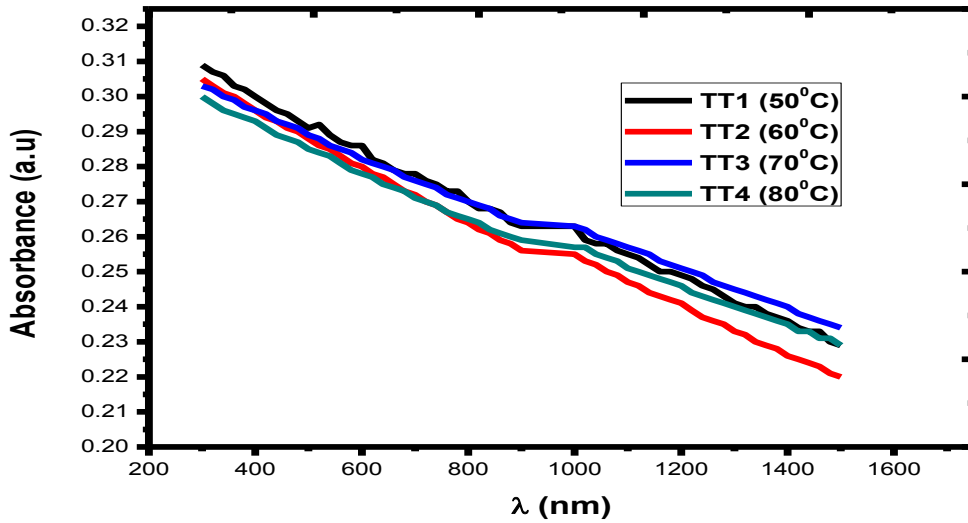


Fig. 5: Plot of absorbance versus wavelength

The optical transmittance of SnZnSe thin films shown in fig. 6 spectral shown that the films grown under the same parametric conditions at varies deposition temperature (50<sup>0</sup>C, 60<sup>0</sup>C, 70<sup>0</sup>C and 80<sup>0</sup>C) for sample TT1, TT2, TT3 and TT4 reveal that as the wavelength of the incident radiation of the material increase the transmittance of the material increases. It was observe that the material grown at 60<sup>0</sup>C transmit above 59% transmittance which reveals the transmittance of

SnZnSe cells grown will be a good material that will absorb energy from the sun [4, 7, 17-19, 23-24] and there is no reported research findings on SnZnSe before this report. SnZnSe cells can also serve as a photovoltaic device and others application in the electronic industry. It was also notices that SnZnSe can be use in mass production of solar cells for the fabrication of lasting solar panel for alternative energy supply.

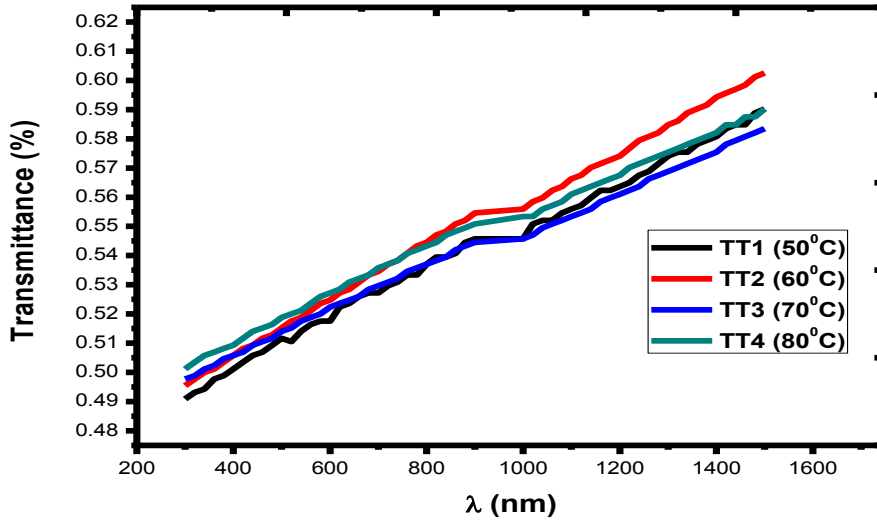


Fig. 6: Plot of transmittance versus wavelength

The optical reflectance of SnZnSe thin films shown in fig. 7 spectral shown that the films grown under the same parametric conditions at varies deposition temperature (50<sup>0</sup>C, 60<sup>0</sup>C, 70<sup>0</sup>C and 80<sup>0</sup>C) for sample TT1, TT2, TT3 and TT4 reveal that as the wavelength of the incident radiation of the material increase the reflectance of the material decreases. It was observed that as temperature of the grown material increase from 50<sup>0</sup>C - 80<sup>0</sup>C the reflectance of the materials decreases

which reveals the reflectance of SnZnSe cells grown will be a good material that will absorb energy from the sun [4, 7, 17-19, 23-24] and there is no reported research findings on SnZnSe before this report. SnZnSe cells can also serve as a photovoltaic device and others application in the electronic industry. It was also notices that SnZnSe can be use in mass production of solar cells for the fabrication of lasting solar panel for alternative energy supply.

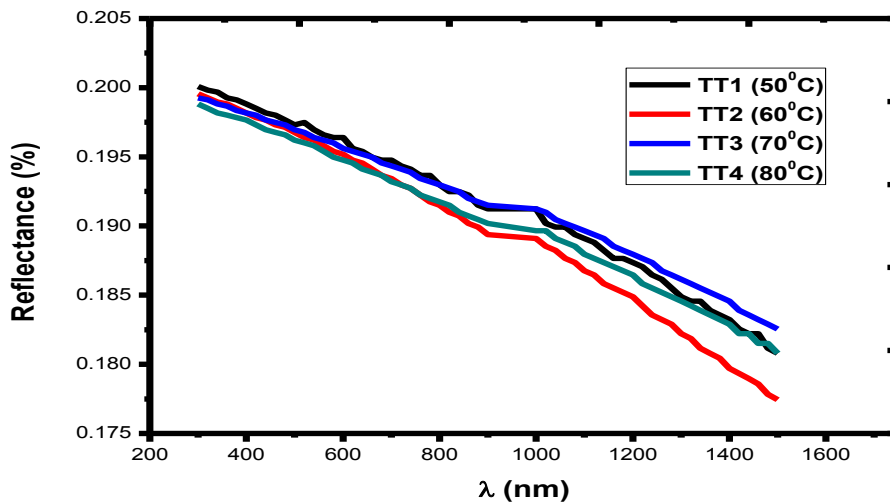


Fig. 7: Plot of reflectance versus wavelength



The optical band gap energy of SnZnSe thin films shown in fig. 8 spectral shown that the films grown under the same parametric conditions at varies deposition temperature (50°C, 60°C, 70°C and 80°C) for sample TT1, TT2, TT3 and TT4 reveal the band gap

energy for the grown SnZnSe thin films which was determine by extrapolating the straight part of the graph of absorption coefficient square against the photon energy to the photon energy axis. From the plot band gap energy is 2.0-2.3eV [4, 7, 17-19, 23-24].

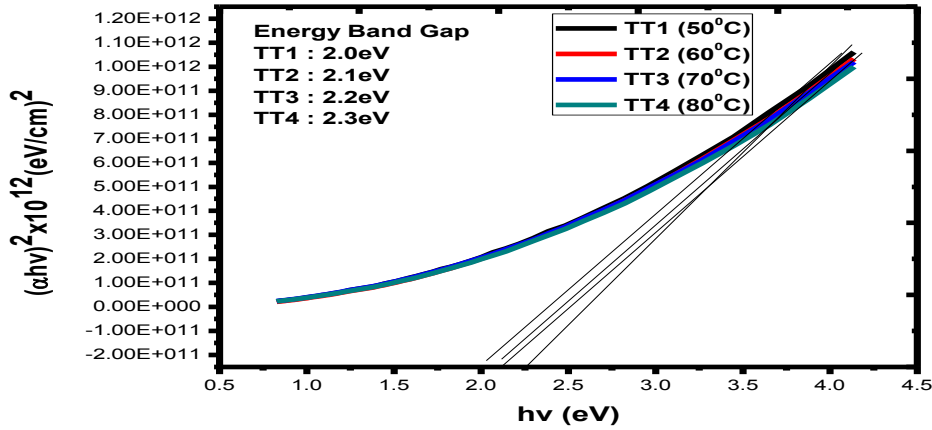


Fig. 8: Plot of absorption coefficient square versus photon energy

The optical refractive index spectral of SnZnSe thin films shown in fig. 9 spectral shown that the films grown under the same parametric conditions at varies deposition temperature (50°C, 60°C, 70°C and 80°C) for sample TT1, TT2, TT3 and TT4 reveal that as the photon energy of the material increase the refractive index increases. It was observe that all the material grown at different pH follow the same thread which reveals the highest refractive index of SnZnSe thin

films and shows that SnZnSe cells grown will be a good material that will absorb energy from the sun [4, 7, 17-19, 23-24] and there is no reported research findings on SnZnSe before this report. SnZnSe cells can also serve as a photovoltaic device and others application in the electronic industry. It was also notices that SnZnSe can be use in mass production of solar cells for the fabrication of lasting solar panel for alternative energy supply.

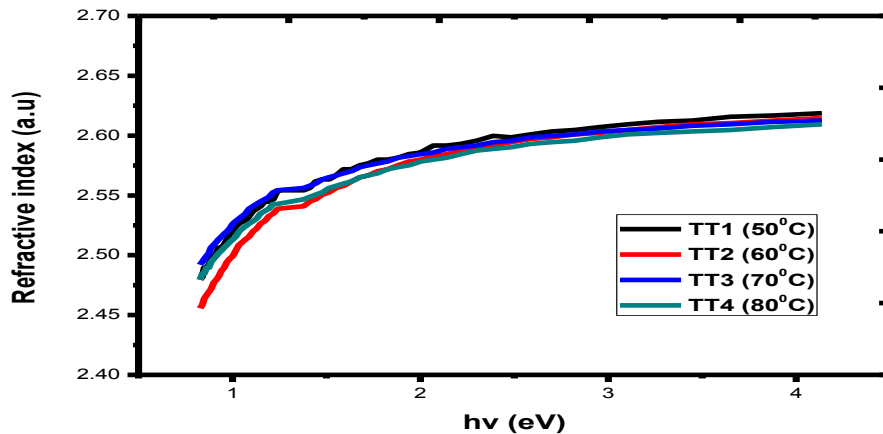


Fig. 9: Plot of refractive index versus photon energy

The extinction coefficient and optical conductivity spectral of SnZnSe thin films shown in fig. 10-11 spectral showed that the films grown under the same parametric conditions at varies deposition temperature (50<sup>o</sup>C, 60<sup>o</sup>C, 70<sup>o</sup>C and 80<sup>o</sup>C) for sample TT1, TT2, TT3 and TT4 reveal that as the photon energy of the material increase the extinction coefficient and optical conductivity increases. It was observe that all the material grown at different pH follow the same thread which reveals the highest extinction coefficient and

optical conductivity of SnZnSe thin films and shows that SnZnSe cells grown will be a good material that will absorb energy from the sun [4, 7, 17-19, 23-24] and there is no reported research findings on SnZnSe before this report. SnZnSe cells can also serve as a photovoltaic device and others application in the electronic industry. It was also notices that SnZnSe can be use in mass production of solar cells for the fabrication of lasting solar panel for alternative energy supply.

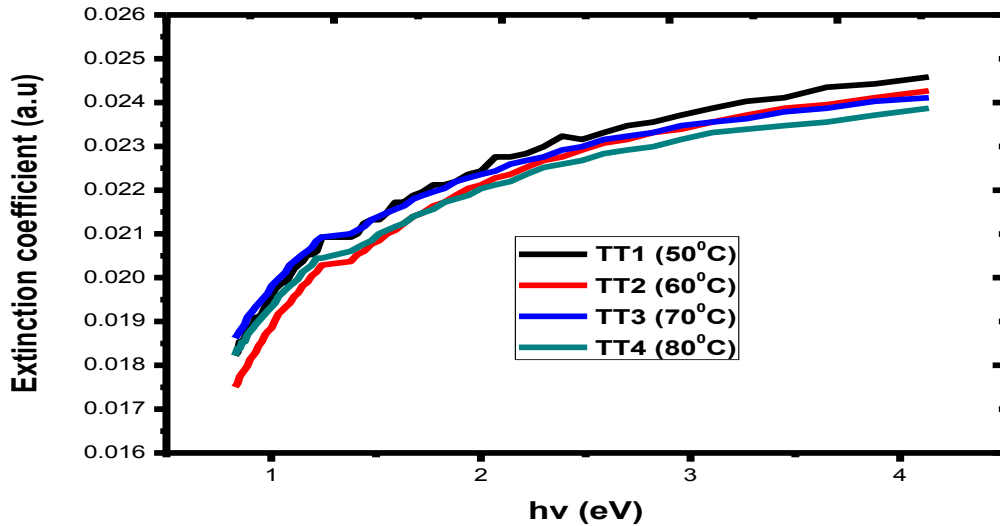


Fig. 10: Plot of extinction coefficient versus photon energy

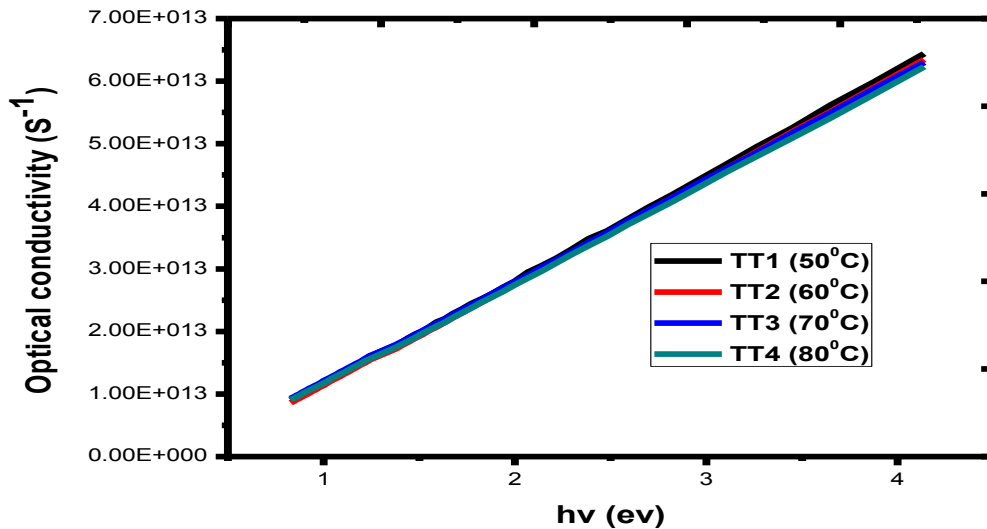


Fig. 11: Plot of optical conductivity versus photon energy

The real and imaginary dielectric constant spectral of SnZnSe thin films shown in fig. 12-13 spectral shown that the films grown under the same parametric conditions at varies deposition temperature ( $50^{\circ}\text{C}$ ,  $60^{\circ}\text{C}$ ,  $70^{\circ}\text{C}$  and  $80^{\circ}\text{C}$ ) for sample TT1, TT2, TT3 and TT4 reveal that as the photon energy of the material increase the real and imaginary dielectric constant increases. It was observed that all the material grown at different temperature follow the same thread which reveals the highest real and imaginary dielectric

constant of SnZnSe thin films and shows that SnZnSe cells grown will be a good material that will absorb energy from the sun [4, 7, 17-19, 23-24] and there is no reported research findings on SnZnSe before this report. SnZnSe cells can also serve as a photovoltaic device and others application in the electronic industry. It was also notices that SnZnSe can be use in mass production of solar cells for the fabrication of lasting solar panel for alternative energy supply.

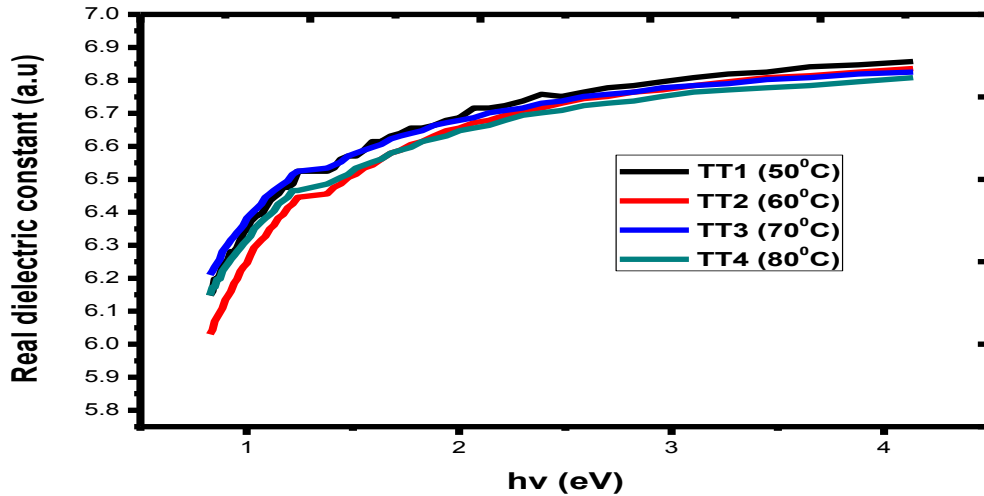


Fig. 12: Plot of real dielectric constant versus photon energy

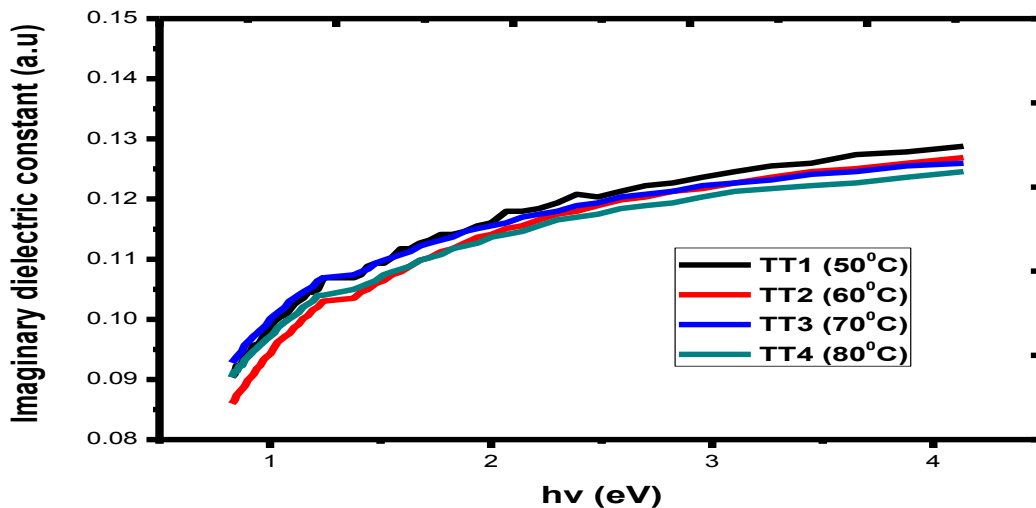


Fig. 13: Plot of imaginary dielectric constant versus photon energy

#### IV. CONCLUSION

Electrochemical deposition technique have been successfully used to grown thin films of SnZnSe. The XRD of the films deposited on FTO substrates at different temperature 50°C, 60°C, 70°C and 80°C shows the reflection peaks at (220), (221), (300), (310), (311), (222) and (320) with the lattice constant of  $a = 7.189 \text{ \AA}$ . SEM shows random distribution of tiny nano-grains on the substrate, the nano grains were observed to agglomerate due to the presence of large free energy characteristic of small particles. As the temperature of the solution increases from 50°C, 60°C, 70°C, and 80°C the nano grain become more packed. The optical band

gap of the deposited material increases from 2.0 – 2.3 eV. The optical absorbance spectra of SnZnSe thin films shown that the films grown under the same parametric conditions and at varying dopant concentration of 50°C, 60°C, 70°C and 80°C for sample TT1, TT2, TT3 and TT4 reveal that as the wavelength of the incident radiation increase the absorbance of SnZnSe thin films decreases. It was also notices that SnZnSe can be use in mass production of solar cells for the fabrication of lasting solar panel for alternative energy supply.

#### ACKNOWLEDGEMENT

We graciously acknowledge the sponsorship of TETFUND office (UNN) through the Needs Assessment Intervention Fund. We also thank Nanosciences African Network (NANOAFNET),

iThemba LABS-National Research Foundation. Also thanks to all staff of Nano Research Group University of Nigeria, Nsukka.

#### REFERENCES

- [1] Mahalingam, T., Kathalingam, A., Lee Soonil, Moon Sunghwan & Kim Deak Yong, (2007), "Studies of Electro synthesized Zinc Selenide Thin Films", Journal of New Material for Electrochemical Systems, 10, 15-19
- [2] Pardo, A. P., Gonzalez, H. G., Castro-Lora, López-Carreño, L. D., Martínez, H. M., Salcedo, N. J. T., (2014). Physical properties of ZnSe thin films deposited on glass and silicon substrates. *J. Phys. Chem. Solid*, 75, 713–725.
- [3] Mahalingam, T., Kathalingam, A., Lee, S., Moon, S., Kim, Y. D., (2007). Studies of Electro synthesized Zinc Selenide Thin Films. *J. New Mater. Electrochemi. Sys.*, 10, 15-19.
- [4] Inran, M., Abida Saleem, Nawazish A. Khan, A. A. Khurram, Nasir Mehmood., (2018). Amorphous to crystalline phase transformation and band gap refinement in ZnSe thin films. *Thin Solid Film*, 11, 1-40. doi.org/10.1016/j.tsf.2018.01.010
- [5] Pentia, E., V. Draghici, G. Sarua, B. Mereu, L. Pintilie, F. Sava and M. Popescu (2004) structural electrical and photoelectrical properties of CdxPb1-xS thin film prepared by chemical bath deposition, *J. Electrochem. Soc.* 151 (11) 729-733
- [6] Sivaraman Chandrasekaran, J. Madhava (2017) Optical, magnetic, and photoelectrochemical properties of electrochemically deposited Eu<sup>3+</sup>-doped ZnSe thin films. *Ionic*. DOI 10.1007/s11581-017-2090-1
- [7] Rajesh, T. Kumar., P. Prabukanthan., G. Harichandran., J. Theerthagiri, Tetiana Tataarchuk., T. Maiyalagan., Gilberto Maia., M. Bououdina., (2017). Physicochemical and electrochemical properties of Gd<sup>3+</sup>-doped ZnSe thin films fabricated by single-step electrochemical deposition process. *Journal of Solid State Electrochemistry*; 27, 254-263
- [8] Sadekar, H. K., Ghule, A. V., Sharma, R., (2013). Nanocrystalline ZnSe thin films prepared by solution growth technique for photosensor application. *Composite Part B*, 44, 553–557
- [9] Samantilleke, A.P., Boyle, M.H., Young, J. & Dharmadas, I.M., (1998), "Growth of n-type and p-type ZnSe thin films using electrochemical techniques for application in large area optoelectronic devices", *Journal of Materials Science: materials in electronics*, 9, 231-235.
- [10] K. Ahn, J. H. Jeon, S. Y. Jeong et al., (2012). Chemical bonding states and atomic distribution within Zn(S,O) film prepared on CIGS/Mo/glass substrates by chemical bath deposition, *Current Applied Physics*, vol. 12, no. 6, pp. 1465–1469.
- [11] D. H. Hwang, J. H. Ahn, K. N. Hui, K. S. Hui, and Y. G. Son, (2012). Structural and optical properties of ZnS thin films deposited by RF magnetron sputtering, *Nanoscale Research Letters*, vol. 7, article 26, pp. 1–13.
- [12] J. P. Bosco, S. B. Demers, G. M. Kimball, N. S. Lewis, and H. A. Atwater, (2012). Band alignment of epitaxial ZnS/Zn<sub>3</sub>P<sub>2</sub> heterojunctions, *Journal of Applied Physics*, vol. 112, no. 9, Article ID 093703.
- [13] S. Yano, R. Schroeder, H. Sakai, and B. Ullrich, (2003). High-electric-field photocurrent in thin-film ZnS formed by pulsed-laser deposition, *Applied Physics Letters*, vol. 82, no. 13, pp. 2026–2028.
- [14] M. W. Huang, Y. W. Cheng, K. Y. Pan, C. C. Chang, F. S. Shieu, and H. C. Shih, (2012). The preparation and cathodoluminescence of ZnS nanowires grown by chemical vapor deposition," *Applied Surface Science*, vol. 261, pp. 665–670.
- [15] G. Xu, S. Ji, C. Miao, G. Liu, and C. Ye, (2012). Effect of ZnS and CdS coating on the photovoltaic properties of CuInS<sub>2</sub>-sensitized photoelectrodes," *Journal of Materials Chemistry*, vol. 22, no. 11, pp. 4890–4896.
- [16] K. Nagamani, N. Revathi, P. Prathap, Y. Lingappa, and K. T. R. Reddy, (2012). Al-doped ZnS layers synthesized by solution growth method, *Current Applied Physics*, vol. 12, no. 2, pp. 380–384.
- [17] G. L. Agawane, S. W. Shin, M. S. Kim et al., (2013). Green route fast synthesis and characterization of chemical bath deposited nanocrystalline ZnS buffer layers," *Current Applied Physics*, vol. 13, no. 5, pp. 850–856.
- [18] Ikhiya, I. L and A. J. Ekpunobi, (2014): Effect of deposition period and pH on Electrodeposition Technique of Zinc Selenide Thin Films. *Journal of Nigeria Association of Mathematical Physics*. 28, 2, 281-288
- [19] Ikhiya, I. L and A. J. Ekpunobi, (2015): Electrical and Structural properties of ZnSe thin films by Electrodeposition

- technique. Journal of Nigeria Association of Mathematical Physics. 29, 325-330
- [20] Hankare, P. P., Chate, P. A., Chavan, P. A., Sathe, D. J., (2008). Chemical deposition of ZnSe thin films: Photoelectrochemical applications', J. Alloys Compd., 461, 623–627.
- [21] Harbeke, G. (1972), In Optical properties of semiconductors F. Abeles (ed) Optical properties of solids, North-holland Pub. Co. Amsterdam, 234-238
- [22] Huang, F., Hou, J., Wang, H., Tang, H., et al., (2016). Impacts of surface or interface chemistry of ZnSe passivation layer on the performance of CdS/CdSe quantum dot sensitized solar cells', Nano Energy, 32, 433–440.
- [23] Senthilkumar, K., Kalaivani, T., Kanagesan, S., Balasubramanian, V., (2012). Synthesis and characterization studies of ZnSe quantum dots. J Mater Sci: Mater Electron 23, 2048–2052.
- [24] Shockley, William (1950). Electrons and holes in semiconductors: with applications to transistor electronics. R. E. Krieger Pub. Co. 234-245.
- [25] Mehta, C., Saini, G. S. S., Abbas, J. M., Tripathi, S. K., (2009). Effect of deposition parameters on structural, optical and electrical properties of nanocrystalline ZnSe thin films. Appl. Surf. Sci., 256, 608–614